Heliyon 6 (2020) e03353

Contents lists available at ScienceDirect

Heliyon

journal homepage: www.cell.com/heliyon

Research article

UHPLC–Q/Orbitrap/MS/MS fingerprinting and antitumoral effects of *Prosopis strombulifera* (LAM.) BENTH. queous extract on allograft colorectal and melanoma cancer models

Fabio Andrés Persia [a,b,1], Mariana Elizabeth Troncoso [a,c,1], Estefanía Rinaldini [a], Mario Simirgiotis [d,e], Alejandro Tapia [f], Jorge Bórquez [g], Juan Pablo Mackern-Oberti [a,h], María Belén Hapon [a,c], Carlos Gamarra-Luques [a,h,*]

[a] *Instituto de Medicina y Biología Experimental de Cuyo (IMBECU), CONICET – Universidad Nacional de Cuyo. Mendoza, Av. Ruiz Leal s/n, Parque General San Martín, CP5500, Mendoza, Argentina*
[b] *Facultad de Ciencias Médicas, Universidad de Mendoza, Boulogne Sur Mer 683, CP 5500, Mendoza, Argentina*
[c] *Cátedra de Química Biológica, Facultad de Ciencias Exactas y Naturales (FCEN), Universidad Nacional de Cuyo, Padre Contreras 1300, CP 5500, Mendoza, Argentina*
[d] *Instituto de Farmacia, Facultad de Ciencias, Universidad Austral de Chile, Campus Isla Teja, 5090000, Valdivia, Chile*
[e] *Center for Interdisciplinary Studies on the Nervous System (CISNe), Universidad Austral de Chile, Valdivia, Chile*
[f] *Instituto de Biotecnología-Instituto de Ciencias Básicas, Universidad Nacional de San Juan, Av. Libertador General San Martín 1109 (O), CP 5400, San Juan, Argentina*
[g] *Laboratorio de Productos Naturales Depto. de Química, Facultad de Ciencias, Universidad de Antofagasta. Av. Coloso S-N, Antofagasta 1240000, Chile*
[h] *Instituto de Fisiología, Facultad de Ciencias Médicas, Universidad Nacional de Cuyo, Centro Universitario, CP5500, Mendoza, Argentina*

ARTICLE INFO

Keywords:
Cancer research
Cell biology
Toxicology
Cell culture
Cell death
Cytotoxicity
Chemotherapy
UHPLC-Q-OT fingerprinting
Phenolic compounds
Colorectal cancer
Melanoma
Antitumoral plants
Prosopis

ABSTRACT

The aqueous extract of the Argentinean native plant, *Prosopis strombulifera* (PsAE), presents cytotoxicity against human cancer cell lines by inducing cytostasis, necrosis and apoptosis; with diminution of clonogenic survival; without genotoxic effects nor oral animal toxicity. Until now, the chemical extract composition and its *in vivo* antitumoral properties remain unknown; these studies are the aim of the current work. The PsAE was characterized by chemical fingerprinting and the metabolome was identified by tandem UHPLC-PDA-HESI-Q-orbitrap® mass spectrometry. Colorectal tumors were induced by DMH administration and melanomas resulted from B16-F0 S.C. cells injection; then, animals were treated orally with PsEA. To correlate *in vivo* results with *in vitro* cytotoxicity, B16-F0 cell were cultured to determine: cell proliferation and viability by dye exclusion assays, MTT and CFSE dilution; cell cycle distribution by flow cytometry; and immunoblotting of $p21^{cip1}$, PCNA, cleaved caspase 3, cleaved PARP and TUBA1A. Based on UHPLC-OT-MS and PDA analysis, twenty-six compounds were identified, including: 5 simple organic acids, 4 phenolic acids, 4 procyanidins, 11 flavonoids, and 2 oxylipins. On C57BL6 mice, PsAE significantly increases the median survival on colorectal cancer and reduces the final volume and weight of melanomas. Over cultured cells, the treatment induce over-expression of p21, cytostasis by G2/M cell cycle arrest and apoptosis; while, on *in vivo* melanomas, treatment up-regulates p21 and slightly decreases PCNA. In conclusion, PsAE is composed by phenolic compounds which demonstrate cytotoxic and antitumoral properties when is orally administrated. Presented results support future research of PsAE as a potential phytomedicine for cancer treatment.

1. Introduction

Cancer consist of a group of illness with a common feature of uncontrolled cellular proliferation determined by several genetic, epigenetic and biochemical causes (Moreno-Sánchez et al., 2014). Despite of the many improvements obtained in cancer treatment, additional answers need to be found to overlap the remained deficiencies. Chemotherapy, as well as conventional treatments against cancer, usually determine unfavorable collateral effects and fails to control cancer progression. The utilization of medicinal plants were proposed as an option

* Corresponding author.
E-mail address: cgamarraluques@gmail.com (C. Gamarra-Luques).
[1] Both authors contributed equally to this work.

https://doi.org/10.1016/j.heliyon.2020.e03353
Received 22 November 2018; Received in revised form 22 March 2019; Accepted 30 January 2020

for the toxic effects determined by synthetic drugs (Rashid et al., 2002). A significant reduction in the undesired effects present in cancer treatment, may be achieved by the use of plant-derived products, among others natural therapies. If well, many anticancer agents were originally described from plants, there are many sources which remain not completely explored (Sultana et al., 2014). In a wide range of climate, Argentina has an abundant and diverse flora. Despite of this, the medicinal properties of native plants were not sufficiently explored; particularly, in relation to cancer. Until now, there are only a few scientific reports about plant antitumoral activities (Mamone et al., 2011).

Prosopis strombulifera (Lam.) Benth, from the Fabaceae family, is a rhizomatous shrub which grows up to 1.5 m height in Argentina, northern and central zones. Locally known as "retortuño", the plant has been ethnopharmacologically used as an astringent, odontalgic, to treat inflammation and diarrhea; scientifically, its anti-bacterial and anti-nociceptive properties have been described. Beneficial biomedical properties of genus *Prosopis* were summarized by Persia et al. (2016).

In relation to cancer, *P. strombulifera* aqueous extract (PsAE) has demonstrated *in vitro* cytotoxic activity against colorectal and mammary adenocarcinoma cancer cell lines (HCT-116 and MCF-7, respectively) by induction of cytostasis, necrosis and apoptosis; with significant diminution in clonogenic survival at LC_{50} doses. By the Ames' test, genotoxic effects of treatment were discarded at the cytotoxic doses used. Moreover, in a BALB/c mice model, no toxicity was evidenced at doses up to 150 mg/animal/day when orally administrated (Hapon et al., 2014).

We hypothesized that PsAE is composed of potential cytotoxic compounds that are able to induce antitumoral effects when are orally administrated. To promote PsAE as a plant-derived compound related to cancer, the objective of this work is to characterize the aqueous extract composition by UHPLC-Q-OT-HESI-MS/MS and to demonstrate its *in vivo* antitumoral properties in mice allograft models of colorectal and melanoma cancers. Additionally, the molecular intermediates of cytotoxic and antitumoral effects were also evaluated.

2. Results and discussion

2.1. UHPLC-Q-OT-HESI-MS/MS analysis of PsAE

The hyphenated chromatographic-spectrometric study of PsAE allowed the detection of 29 peaks (Figures 1A and 1B), where identification of 26 compounds was possible, including: 5 simple organic acids, 4 phenolic acids, 4 procyanidins, 11 flavonoids, and 2 oxylipins (Table 1). The full metabolome identification is explained below:

Simple organic acids: xylonic, citric, isocitric, grisenilosidic and tuberonic acid glucoside; peaks 2-4, 12 and 14, respectively.

Phenolic acids: protocatechuic, piscidic, salicylic and marmesin; peaks 6, 7, 24 and 29, respectively.

Procyanidins: flavanols gallocatechin and epigallocatechin, catchin and procyanidin B1; peaks 8, 11, 13 and 15, respectively.

Flavonoids: daidzein 7-O-glucuronide, neoeriocitrin, kaempferol 3-O-neohesperidose, myricitrin 3-O-glucoside, rhoifolin, rutin, kaempferol glucoside, kaempferol rhamnoside, naringoside, formononetin 7-O-6ácetylglucoside, kaempferol; peaks 5, 9, 10, 16-22 and 25, respectively. Some compounds were identified as flavanones (l max 281 nm), other as isoflavones (l max 281 nm) and other as flavonols (l max 254–354 nm).

Oxylipins: unsaturated fatty acids trihydroxylinoleic acid and trihydroxyoctaenoic acid; peaks 26 and 28, respectively.

The chemical characterization of PsAE, identified 26 compounds; at least, 12 of them had been previously reported as cytotoxic. While, protocatechuic acid (Tsao et al., 2014), marmesin (Dong et al., 2018), rutin (Asfour and Mohsen, 2017), kaempferol, kaempferol glucoside and kaempferol rhamanoside (Wang et al., 2018) were described as isolate active compounds against cancer cells; citric acid, gallocatechin, epigallocatechin, procyanidin B and rhoifolin were reported as component of natural extracts with cytotoxic activity (Koyuncu, 2018; Navarro et al., 2017; Radan et al., 2017; Tremocoldi et al., 2018). The concurrence of the mentioned compounds into PsAE ensures its anticancer effects and promotes new research concerning its biological properties.

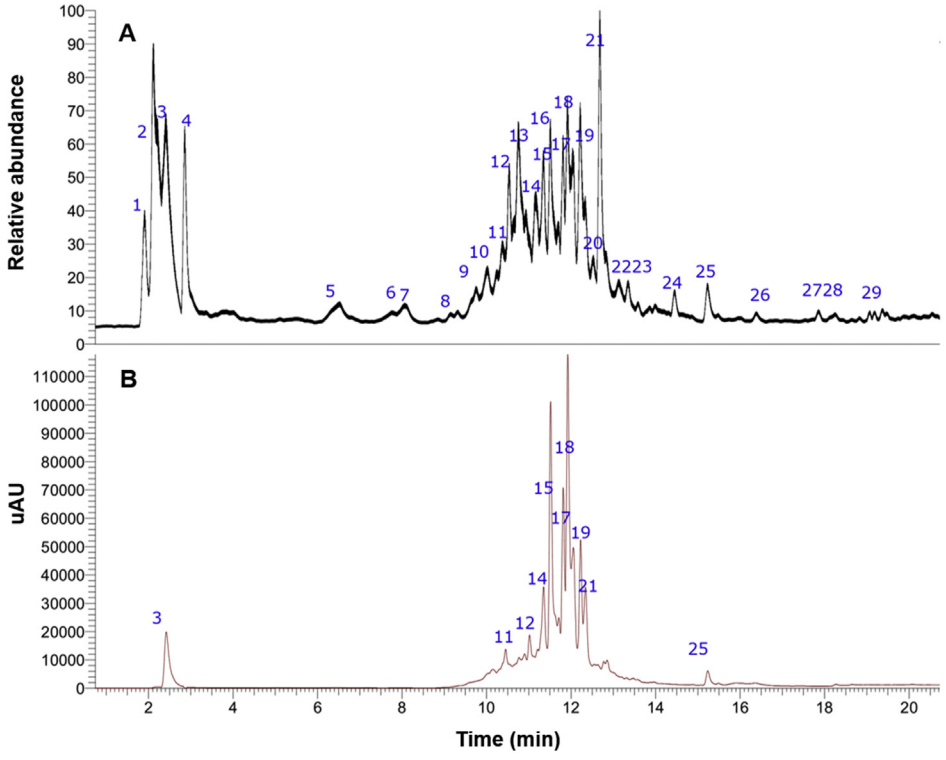

Figure 1. UHPLC-Q-OT-HESI-MS/MS fingerprints of PsAE. A. The total Ion Current (TIC) chromatogram. B. The UV-vischromatogram at 330 nm.

Table 1. High resolution UHPLC PDA-Q orbitrap identification of metabolites in the PsAE.

Peak#	Retention time (min.)	UV max	Tentative identification	Elemental composition [M-H]	Theoretical mass (*m/z*)	Measured mass (*m/z*)	Accuracy (δppm)	MSn ions (δppm)
1	1.87	-	Unknown			272.95877		
2	2.11	-	Xylonic acid	$C_6H_8O_7$-	165.03984	165.03936	2.88	
3	2.41	-	Citric acid	$C_6H_8O_7$-	191.01932	191.01863	3.44	
4	2.86	-	Citric acid isomer	$C_6H_8O_7$-	191.01929	191.01863	3.44	
5	5.29	280	Daidzein 7-O-glucuronide	$C_{21}H_{17}O_{10}$-	429.08162	429.08270	2.51	
6	6.50	305-350	Protocatechuic acid	$C_7H_5O_4$-	153.01868	153.01824	2.88	
7	7.69	271	Piscidic acid	$C_{11}H_{11}O_7$-	255.05090	255.04993	3.81	
8	8.08	271	Gallocatechin	$C_{15}H_{13}O_7$-	305.06671	305.06558	3.71	289.07169 (catechin)
9	9.90	281	Neoeriocitrin (eriodictyol 7 neohesperidoside)	$C_{27}H_{31}O_{15}$-	595.16614	595.16575	0.65	
10	10.03	255-365	Kaempferol 3-O-neohesperidose	$C_{30}H_{25}O_{13}$-	593.12952	593.12897	0.92	285.0610 (kaempferol)
11	10.36	271	Epigallocatechin	$C_{15}H_{13}O_7$-	305.06674	305.06558	3.81	289.07169 (catechin)
12	10.55	295-345	Grisenilosidic acid	$C_{17}H_{21}O_{12}$-	417.10379	417.10275	2.46	177.01866
13	10.77	271	Catechin	$C_{15}H_{13}O_6$-	289.07178	289.07066	0.44	125.02163
14	11.14	198	Tuberonic acid glucoside	$C_{18}H_{27}O_9$-	387.16496	387.16611	0.48	309.13739, 261.08792
15	11.34	271	Procyanidin B1	$C_{3}oH_{25}O_{12}$-	577.13434	577.13404	0.48	289.07175 (catechin)
16	11.69	255-355	Myricitrin 3-O-glucoside	$C_{17}H_{19}O_9$-	479.08202	479.08307	2.19	271.02454
17	11.81	269	Rhoifolin	$C_{27}H_{30}O_{14}$-	577.15518	577.15570	0.89	
18	11.90	255-354	Rutin	$C_{27}H_{29}O_{16}$-	609.14611	609.14532	0.41	271.02472
19	12.21	255-365	Kaempferol glucoside	$C_{21}H_{19}O_{11}$-	447.09320	447.09219	2.26	285.04019 (kaempferol)
20	12.06	270-334	Kaempferol rhamnoside	$C_{21}H_{19}O_{10}$-	431.09833	431.09727	2.44	285.0610 (kaempferol)
21	12.71	255-325	Naringoside	$C_{27}H_{31}O_{14}$-	579.17083	579.17083	2.96	
22	13.11	310	Formononetin 7-O-6ácetylglucoside	$C_{24}H_{23}O_{10}$-	471.12979	471.12857	2.58	
23	13.35	220	Unknown	$C_{18}H_{33}O_5$-	341.23837	341.23678	4.67	
24	14.47	240	Hydroxybenzoic acid (salicilic acid)	$C_7H_6O_3$-	137.02373	137.02332	2.96	
25	15.25	255-365	Kaempferol	$C_{34}H_{29}O_{15}$-	285.04046	285.04053	0.24	
26	17.86	220	Trihydroxylinoleic acid	$C_{18}H_{31}O_5$-	327.21660	327.21331	3.39	
27	16.45	220	Unknowrn	$C_{18}H_{33}O_5$-	341.23837	341.23678	4.67	
28	17.98	220	Trihydroxyoctaenoic acid	$C_{18}H_{33}O_5$-	329.23346	329.23225	3.57	
29	19.38	254-354	Marmesin	$C_{14}H_{19}O_4$-	245.08173	245.08084	3.63	

Many natural derivatives are actually used to treat chronic diseases like cancer; these products are selected mainly for safety, availability, tolerance and its biological activity (Singh, 2007). In general, previous reports indicate that phytochemicals bring a higher protection acting combined than isolated (Malongane et al., 2017). Therefore, described constituents of PsAE support its cytotoxicity, potency and efficiency against a wide range of cancer cell; and promote their use as phytomedical agents.

2.2. Evaluation of antitumoral properties of PsAE on mice

Because *in vivo* antitumoral properties of PsAE were not previously reported, to probe the extract capability of interfere with *in vivo* tumor progression, the present work shows the extract activity on two different models of cancer. One of them, are the colorectal tumors induced by the procarcinogen compound DMH; and the other, are the melanomas induced by subcutaneous injection of B16-F0 cells. Both are considered as allograft models of cancer in mice and, in the two cases, treatment was administrated at the major no toxic doses reported of 150 mg/animal/day (Hapon et al., 2014).

2.2.1. PsAE antitumoral activity: median survival determination on DMH induced colorectal cancer

To study the *in vivo* activity of PsAE against colorectal cancer, tumors were developed by DMH administration in BALB/c mice. A control group of animals, without DMH tumor induction, were used. These animals presented 100% survival during the experimental time (52 weeks), without any signs of tumor development. On the other hand, all animals DMH treated evidenced humane endpoints criteria related to colorectal cancer growth and were euthanized in consequence. Animals weight loss during experimental time was always between 5 to 8 %. The euthanasia criteria presented were anal tumor protrusion or anal bleeding. Necropsy evidenced colorectal polyps in all DMH treated animals, with no differences in the number of polyps between control and treated groups (18-24 polyps/animal). The diagnosis of colorectal adenocarcinoma was confirmed by histology. Kaplan-Meier analysis indicates that PsAE treated animals show the highest median survival, 34.5 weeks, whereas values of the not treated group and 5Fu treated were 24 and 27 weeks, respectively (Figure 2A). Survival differences between PsAE treated animals were significant in relation to the control group (Mantel Cox test, $p < 0.0001$) and 5Fu group (Mantel Cox test, $p = 0.0030$). The presented data demonstrate that PsAE, orally administrated, interferes with colorectal cancer progression. However, by these experiments, it is not possible to determine if plant derived active compounds act by hematological (systemic) or intraluminal (topic) ways.

2.2.2. PsAE antitumoral activity: systemic antimelanoma activity in allograft B16-F0 induced tumors

To investigate whether PsAE acts systemically to prevent melanoma progression, the extract was administrated orally in drinking water from day 1–22, after subcutaneous implantation of B16-F0 melanoma cells in C57BL6wt mice. Two additional groups were added; a control group without any treatment; and the 5Fu treated group. All animals developed tumors, which were histologically confirmed. At the end of the experiment, day 22 after cells inoculation, the mean weight and volume of tumors excised from PsAE treated mice were significantly lower than the control group (Figure 2B). While control tumors weight was 2.389 ± 0.605 g, in PsAE group was significantly lower, 0.736 ± 0.190 g ($p =$

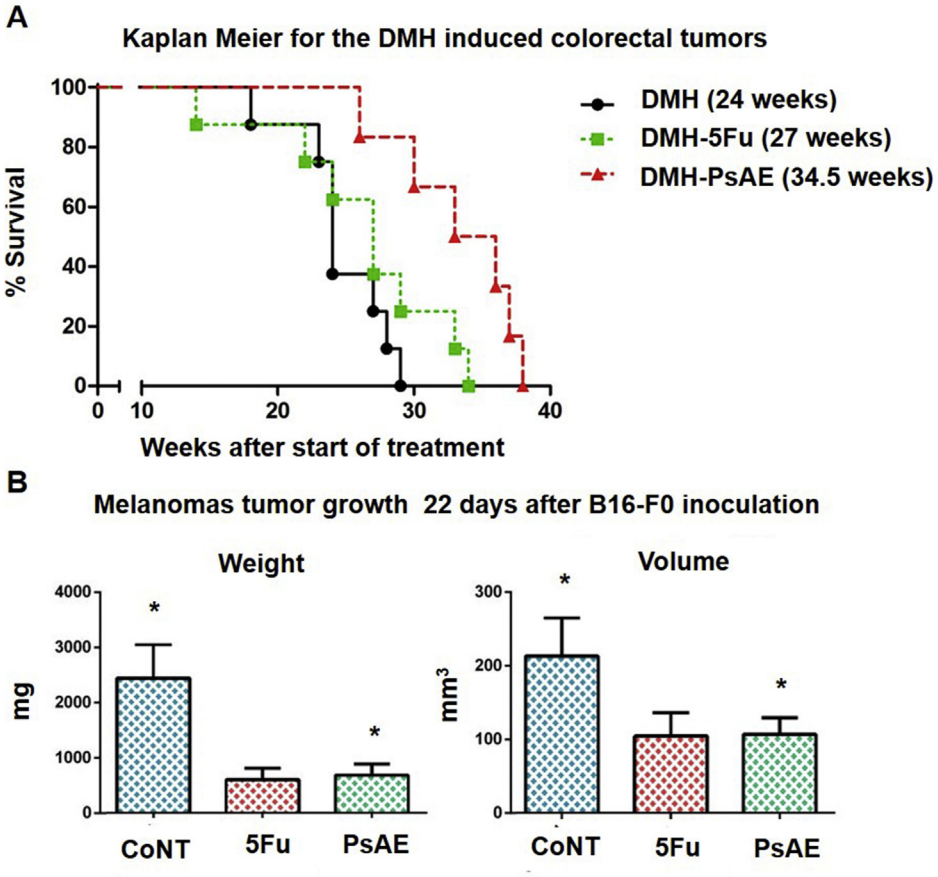

Figure 2. PsEA antitumoral effects in colorectal and melanoma tumors. A. Kaplan-Meier analysis of survival proportions in BALB/c mice. Median survival of each animal group is indicated. B. Weight and volume comparison in C57BL6wt mice allograft melanoma tumors. DMH: Dimethylhydrazine. CoNT: Control no treated. 5Fu: 5-Fluoracile. PsAE: *P. strombulifera* aqueous extract. *: indicates significant differences between CoNT and PsAE groups (ANOVA, Fisher LSD test, $p \leq 0.05$).

0.0204). When the final volume was analyzed, controls reach final volumes of 219 ± 47.9 mm^3 whereas PsAE treated tumors reached a significantly diminished volumes of 101.7 ± 20.7 mm^3 ($p = 0.0306$). The 5Fu treated group showed a final weight of 0.612 ± 0.50 g and a volume of 99 ± 27.8 mm^3; no significant differences with PsAE values were found. Altogether, the presented results indicate the capability of PsAE to interfere with melanoma growth *in vivo* and demonstrate the systemic bioavailability of the active plant derived compounds.

2.3. *In vitro evaluation of PsAE cytotoxic effects*

To determine how PsAE exerts its antitumoral activity, B16-F0 murine melanoma cancer cells were cultured and studied in a dose-response experimental design.

2.3.1. *PsAE induce cytotoxic effects by affection of proliferation and viability*

Cell number and viability were quantified by dye exclusion assay with trypan blue, after 48 h of treatment. *In vitro* activity was quantified by IC_{50} and LC_{50} determination, the chemotherapeutic agent 5Fu was used as positive control. For PsAE, the estimated IC_{50} was 2.44 ± 0.18 μg/ml and the LC_{50} was 9.01 ± 0.22 μg/ml; whereas the calculated values for 5Fu were 0.12 ± 0.01 and 18.40 ± 1.04 μg/ml, respectively (Figures 3A and 3B). The obtained results evidence the capability of the PsAE to induce cytotoxicity in a dose-response manner by affection of cells proliferation and viability.

Next, we examined the morphological features in fixed and stained B16-F0 cells, 48 h treated, with IC_{50} and LC_{50} PsAE concentrations (2.4 and 9 μg/ml, respectively), in comparison with not-treated controls. The extract reduced cell density, caused rounding nucleus and enlarged cell cytoplasms; all changes were evident in a dose-response manner (Figure 3C).

To confirm the effects induced by PsAE treatment in cell proliferation two additional techniques were applied. By assessing cell metabolic activity with the MTT assay, we demonstrate how increased doses of PsAE induce growth inhibition in a dose-response manner (Figure 4A). In fact, the changes determined by quantification of the mitochondrial activity with PsAE and 5Fu, were able to induce the same proliferative changes to those calculated by the dye exclusion assay.

In addition, cell proliferation was studied by CFSE dilution in control and treated cells. Figures 4B, 4C and 4D show how CFSE fluorescence in control no treated cells (CoNT) results diminished in successive mitotic divisions. Similarly as was observed in dye exclusion and MTT assays, PsAE and 5Fu, used at IC_{50} and LC_{50} concentrations, interfere with normal cell division evidenced by increased CFSE fluorescence after 48 h of treatment (Figures 4B, 4C and 4D).

2.3.2. *PsAE induce G2/M cell cycle arrest*

To elucidate how PsAE effects the cell cycle progression, we assessed cell cycle distribution by flow cytometry analysis in B16-F0 cells (Figures 5A and 5B). Cells were incubated in the presence of PsAE for 24 h at IC_{50} and LC_{50} concentrations (2.4 and 9 μg/ml, respectively), untreated control cells were also assayed. As shown in Figure 5, treatment with PsAE induced a marked G2/M arrest with a concurrent reduction of cell population on G1 in both treated groups. Also, at the IC_{50} concentration was observed an augmentation of >4N fraction, which represents cells with higher DNA content than tetraploid cells. Moreover, a slight increase in hypo-diploid DNA content (SubG1 phase) was observed at LC_{50} concentration; which indicates apoptosis as a cell death mechanism

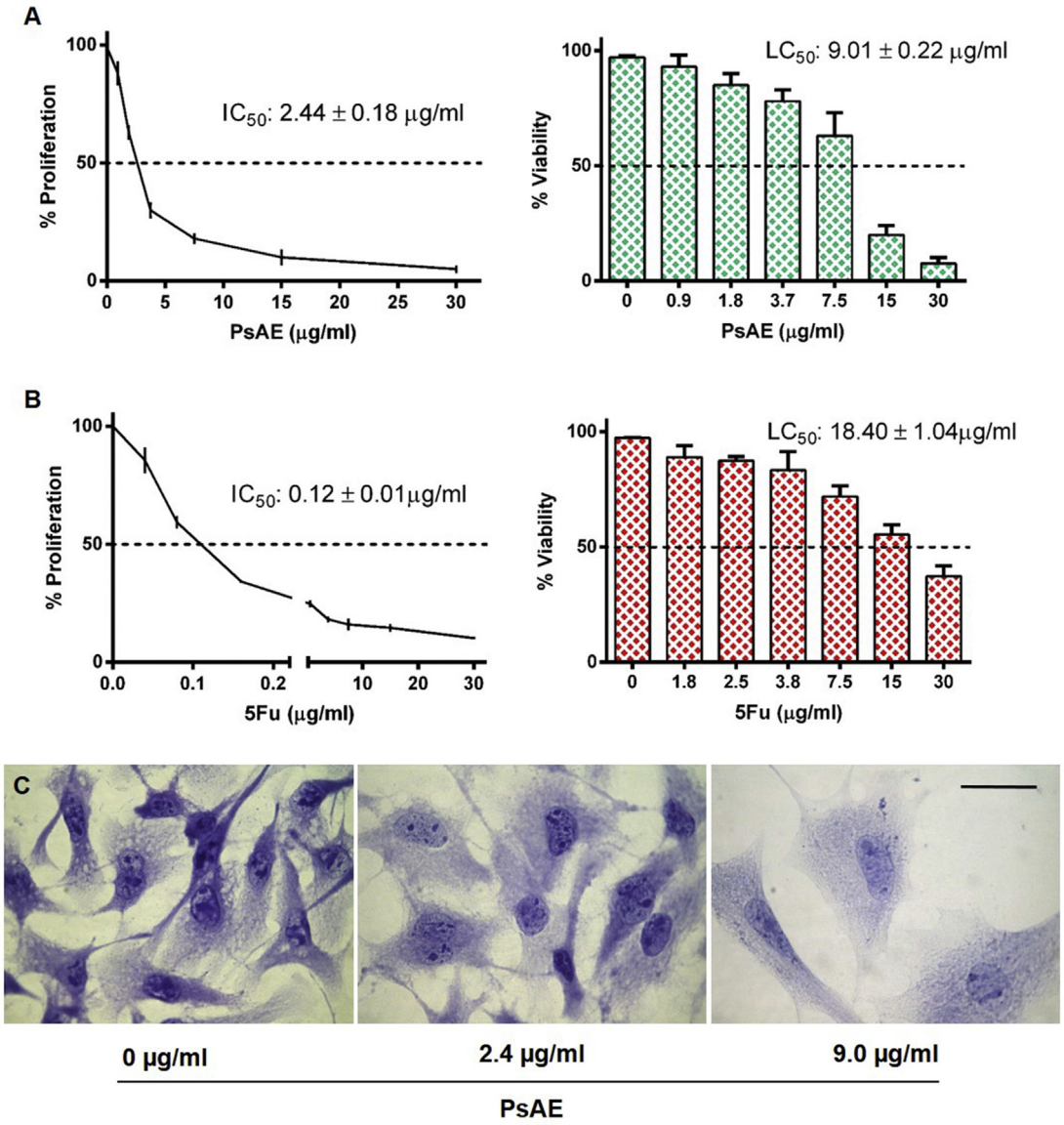

Figure 3. Determination of *in vitro* PsAE cytotoxic effects. A. Dye exclusion assay of *in vitro* B16-F0 cell line after 48 h treatment with PsAE in a dose-response experimental design. B. Proliferation and viability changes induced by 5Fu on B16-F0 cells. C. Morphological changes induced by PsAE treatment at IC_{50} and LC_{50} (2.4 and 9 µg/ml, respectively) concentrations compared with not-treated control cells. Size bar corresponds to 50µm. In A and B, IC_{50} and LC_{50} were statistically calculated by a sigmoidal dose-response analysis using Prism® 6.0.

involved (Gamarra-Luques et al., 2012). Presented results demonstrated that PsAE interferes with cell cycle progression mainly by the arrest in G2/M phase and augmentation of >4N cells DNA content; these mentioned cell cycle distribution changes are similar to compounds which exert cytotoxicity by mitosis interference (Dolečková et al., 2012; Liu et al., 2016; Yu et al., 2017; Zhao et al., 2019).

2.3.3. *PsAE induce changes in protein expression related to the presence of cytostasis and apoptosis*

Protein expression was determined to study the cytostatic and lethal effects of PsAE on B16-F0 cultured cells (Figs. 6A and 6B). Three independent assays, after 24 h of treatment at 0 µg/ml, IC_{50} and LC_{50} PsAE concentrations (2.4 and 9 µg/ml, respectively), were done. In IC_{50} treated cells, in respect to control not-treated cells (CoNT), the cyclin-dependent kinase inhibitor $p21^{cip1}$ (p21) significantly increases ($p = 0.0273$), and cleaved caspase 3 increases significantly ($p = 0.0500$); these results are consistent with cell cycle arrest associated with growth inhibition. At lethal doses, compared with controls, the expression of p21 was increased ($p = 0.0489$), cleaved caspase 3 was significantly increased (0.0007); also, detection of cleavage in poly ADP ribose polymerase (cPARP) revealed the presence of apoptosis and its overexpression showed a significant increase ($p = 0.0081$); while PCNA was significantly reduced ($p = 0.0395$). Altogether, molecular markers indicate that cytostasis and lethality are induced *in vitro* by PsAE treatment mediated by a p21 related mechanism.

2.4. *Molecular confirmation of PsAE antitumoral systemic effects*

To correlate the molecular changes evidenced *in vitro* by PsAE treatment, with the antitumoral effects demonstrated in allograft melanomas after subcutaneous B16-F0 cells inoculation, the expression of cytostasis and apoptosis related proteins were analyzed.

After 22 days of the melanoma induction, tumors of the animals orally treated with 150 mg/day of PsAE were compared to the tumors resulting from untreated animals (Figs. 7A and 7B). When the cell cycle arrest related proteins were studied, p21 significantly increases ($p = 0.0133$) and PCNA did not diminish significantly in the PsAE treated group. The apoptosis related protein cleaved PARP, was not detected in PsAE, nor in

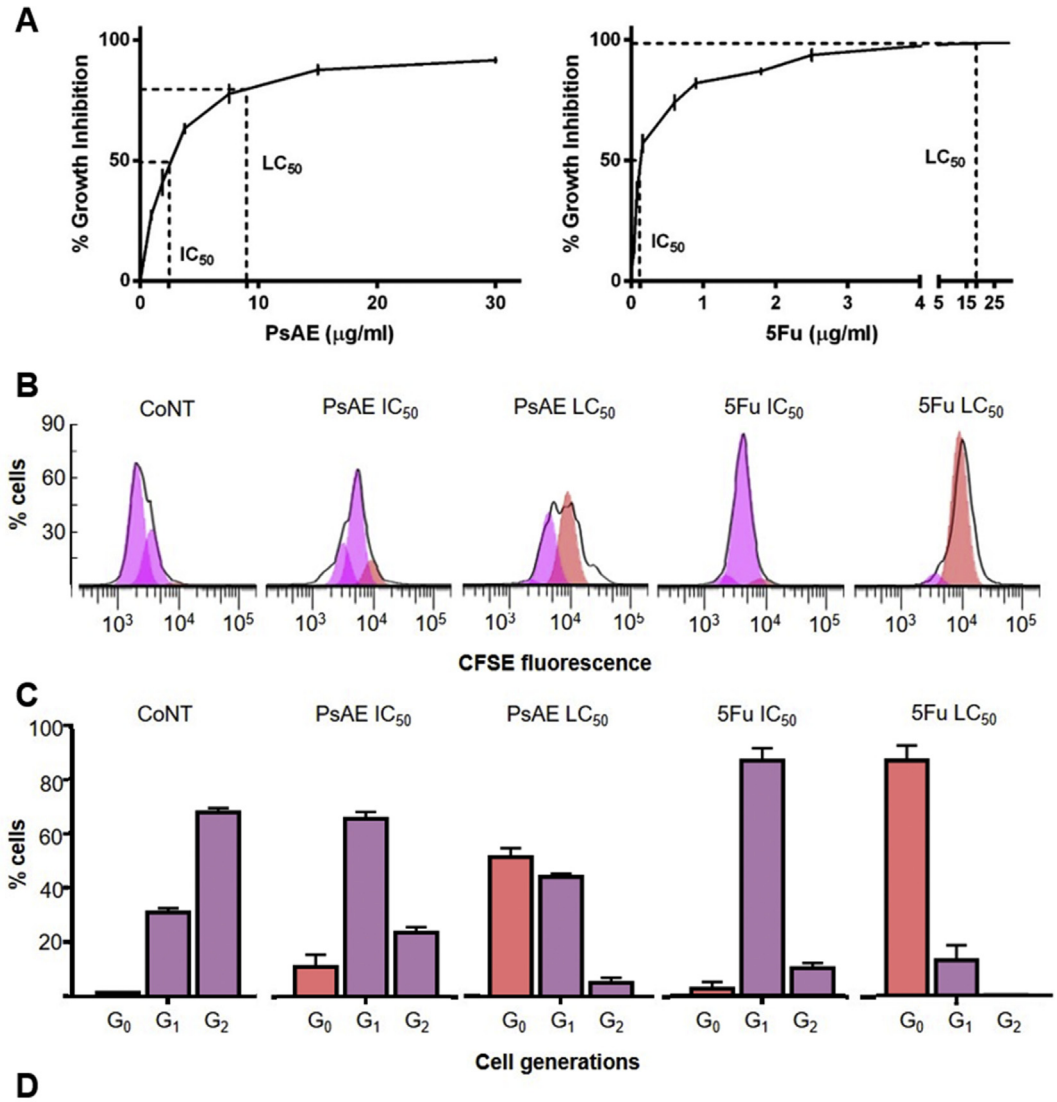

D

Group		Control	PsAE IC_{50}	PsAE LC_{50}	5Fu IC_{50}	5Fu LC_{50}
% Cells by Generation	G_0	1.4 ± 0.3	10.9 ± 0.3	51.2 ± 1.5	2.8 ± 0.2	86.8 ± 2.6
	G_1	30.9 ± 1.8	65.6 ± 1.5	43.9 ± 0.6	86.9 ± 2.1	13.1 ± 2.6
	G_2	67.7 ± 2.1	23.5 ± 2.3	5.0 ± 0.9	10.3 ± 1.2	0.1 ± 0.0
CFSE fluorescence intensity	Mean	2446 ± 142	5844 ± 235	9348 ± 417	5083 ± 196	10869 ± 311
	Median	2080 ± 108	5246 ± 194	7033 ± 298	4633 ± 163	9884 ± 209

Figure 4. Proliferation changes in B16-F0 cell line. A: Growth inhibition percentage (%) in a dose response MTT proliferation assay. B, C and D: Flow cytometric analysis of cell division by dilution of CFSE. In B, CFSE representative histograms of control and treated cells (black line), pink solid histograms show undivided cells (generation 0, G0) and purple histograms represent the following generations (G1 and G2). Panel C display Percentage (%) of cells distribution by generation in different treatment paradigms. In D, tabular results and statistical comparison of cells distribution percentage (%) by generation, and mean/median fluorescence intensity of total cells. CoNT = Control No Treated; PsAE IC_{50} = 2.44 µg/ml; PsAE LC_{50} = 9.01; 5Fu IC_{50} = 0.12 µg/ml and 5Fu LC_{50} = 18.40 µg/ml. Treatments were performed for 48 h. Results are expressed as mean ± SEM, of three independent assays by triplicated and were compared by one-way ANOVA followed by Fisher LSD test. *: indicate significant differences ($p < 0.0001$) respect to control group.

the control group (data not shown). In accordance to the explored molecular markers expression, it is possible to affirm that *in vivo* treatment with oral PsAE exerts antitumoral actions by cytostasis, without apoptosis mediated cell death. Moreover, in the used animal model in which the treatment was orally administrated, the systemic PsAE should reach bioactivity levels that are comparable with the IC_{50} concentration assayed *in vitro*.

As has been described in other natural compounds with systemic antimelanoma actions, PsAE treatment may activate multiple target pathways. Diverse compounds that induced G2/M cell cycle arrest

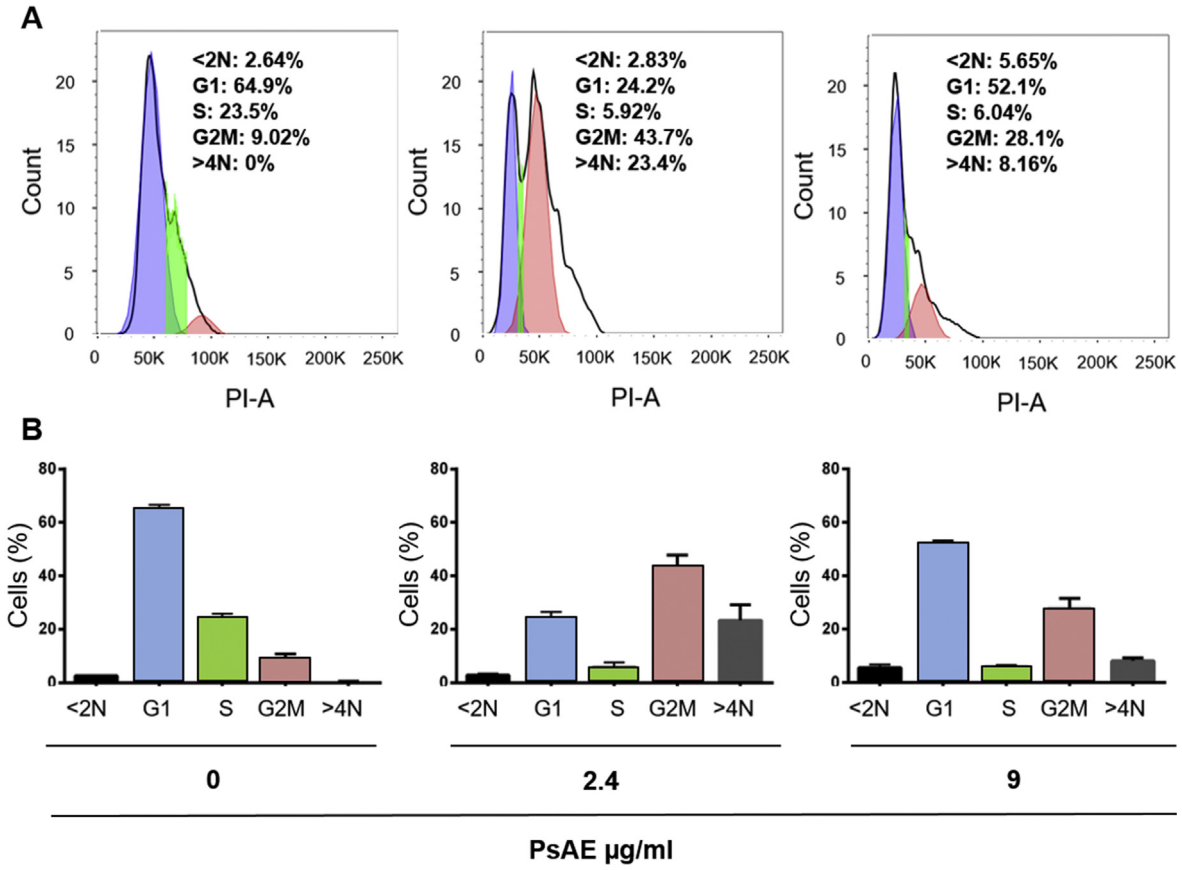

Figure 5. Cell cycle analysis of B16-F0 cells. A. Flow cytometric histograms show the DNA content and the corresponding percentages of cell cycle distribution in control, IC_{50} and LC_{50} (0, 2.4 and 9 µg/ml, respectively) PsAE concentrations. B. Cell cycle distribution in bars. Cytometric analysis was performed after 24 h treatment. Mean ± SEM of 3 independent assays by triplicate are presented.

accompanied by p21 up-regulation such as: genistein (obtained from soybeans), α-santalol (from *Santalum album*) and allyl-sulfides (obtained from garlic), among others (Ravindranath et al., 2004; Wang et al., 2012; Zhang and Dwivedi, 2011), have been reported. As PsAE, the mentioned compounds were described to act by the control of proliferative signals, altering cell cycle regulatory proteins and complexes, determining its proved efficacy accompanied by null collateral effects. Moreover, the multiple molecular targets involved, make able to explore and exploit the synergistic combinations with other current available chemotherapeutic agents, to promote the use of natural derived compounds as valuable complementary treatments against cancer.

3. Conclusions

The present study demonstrates that the PsAE UHPLC fingerprint is composed by phenolic compounds; which, at least 12 of them, were previously reported as cytotoxic against cancer cells; supporting, at least in part, the potential antitumoral activity of this plant. When PsAE is orally administrated, prevents tumor progression *in vivo* by a significant increase of the mice median survival with allograft colorectal tumors and cause diminution of the tumor growth in subcutaneous B16-F0 induced melanomas. The *in vitro* dose-response assays performed in this work show that PsAE induces G2/M cell cycle arrest and apoptosis in B16-F0 cells, determining a significant over expression of the cyclin-dependent kinase inhibitor $p21^{cip1}$. Finally, the molecular study of the mice induced melanomas indicates that systemic available plant derived compounds cause cytostasis with over expression of $p21^{cip1}$ but not apoptosis. Altogether, the findings of the current work demonstrated the antitumoral activity of PsAE when is orally administrated. Further research are needed in order to explore its effect on the regulation of related signal pathways to support the plant extract use as complementary medicine for cancer treatment.

4. Materials and methods

4.1. Plant material and aqueous extract preparation

P. strombulifera was collected in February 2016 in 33° 44′10″ S, 68° 21′ 30.5″ W (Lavalle County, Mendoza, Argentina). Identified as MERL 61824 a voucher specimen is deposited in the Mendoza Ruiz Leal herbarium. To obtain PsAE, leaves were autoclaved in distilled water, 50 g/500 ml, for 1 h. After, solids separation by paper filtration, decoction was boiled until volume reach 50 ml. Before use, crude extract was sterilized by passing through a 0.22 µm pore size filter. The concentration (w/v) was estimated by the ratio between the weight of the leaves, expressed in grams, and the final volume obtained at the end of the preparation: 50 g/50 ml = 1 g/ml.

4.2. Detection and identification of PsAE compounds by UHPLC-Q-OT-HESI-MS/MS

By UHPLC-Q-OT-HESI-MS/MS PsAE compounds were identified and quantified. Collision and damping gas was performed by a Thermo Scientific Dionex Ultimate 3000 UHPLC system (Thermo Fisher Scientific, Germany), controlled by the Chromeleon 7.2 Software; hyphenated with a Thermo high resolution Q Exactive focus mass spectrometer (Thermo, Bremen, Germany). A Zefiro nitrogen generator (Clantecnologica, Sevilla, Spain) was used to obtain pure nitrogen (>99.999%). Equipment calibration and parameters settings were performed as was previously reported by Simirgiotis et al. (2016). The chromatography parameters

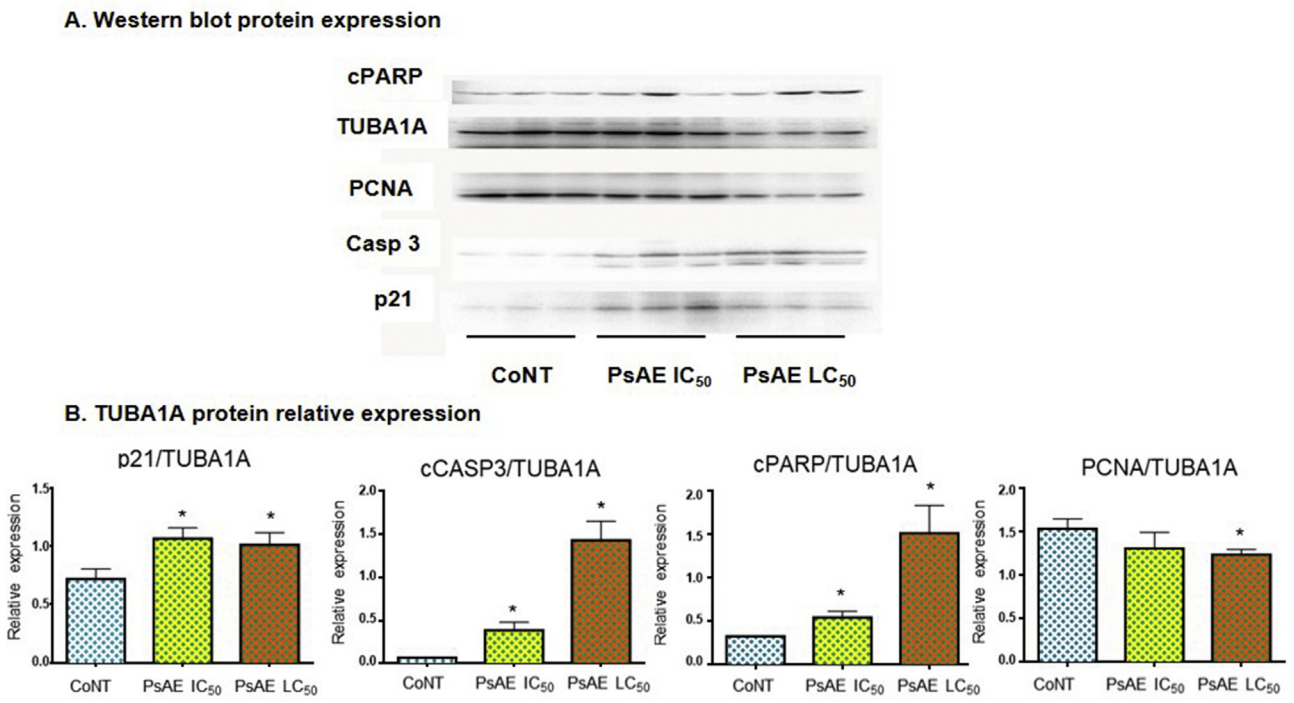

Figure 6. Western blot analysis of cultured B16-F0 cells. A. After 24 h, protein expression of control, IC_{50} and LC_{50} PsAE treated cells (0, 2.5 and 9 μg/ml, respectively) are presented. B. Relative expression of p21, caspase 3, PCNA and cPARP with respect to TUBA1A are expressed in terms of mean ± SEM of three assays by triplicated. Results were compared by one-way ANOVA followed by Fisher LSD test. *: indicate significant differences ($p \leq 0.05$) respect to control group. Full, non-adjusted images of cPARP blot is provided in Supplementary Figure 1; TUBA1A (upper line) and PCNA (lower line) are provided in Supplementary Figure 2; caspase 3 is provided in Supplementary Figure 3; and p21 is provided in Supplementary Figure 4.

were: UHPLC C18 column (Acclaim, 150 mm * 4.6 mm ID, 5 μm, Restek Corporation, Bellefonte, PA, USA), at 25 °C. Detection settings were at 254, 280, 320, and 440 nm, and the PDA record was from 200 to 800 nm. Mobile phases used were: (A) 1% formic acid aqueous solution and (B) acetonitrile with 1% formic aqueous solution. The gradient program and time (min, % of B) was: (0.00, 5); (5.00, 5); (10.00, 30); (15.00, 30); (20.00, 70); (25.00, 70); (35.00, 5), and column equilibration for 12 min. The injection volume was 10 μl and the flow rate fixed at 1 ml/min. Samples and standards were dissolved in methanol and kept in the autosampler at 10 °C. The MS parameters were as follows: the HESI II and other parameters for the Q-orbitrap instrument were optimized as previously reported (Jiménez-González et al., 2018).

4.3. Animals and in vivo treatments

All animals were maintained in a controlled light (6:00 AM to 10:00 PM) and room temperature (22–24 °C. Drinking liquids and mice chow (Cargill, Argentina) were available *ad libitum*. *In vivo* treatment was performed by diluting PsAE (150 mg/animal/day) in drinking water. Intraperitoneal 5Fu was the chemotherapeutic control treatment administrated, at 30 mg/kg/week, until animal sacrifice.

To study the animal median survival after DMH colorectal tumor induction were used BALB/c males, 6 weeks old at the onset of treatment, bred in our Institute. Four groups were separated of 10 animals each. Group 1 was considered as survival control group and did not receive treatments. In the other 3 groups was performed the colorectal tumor induction by S.C. administration of DMH, 20 mg/kg/week, for 22 weeks (Persia et al., 2017). In animals of group 2 (DMH), only tumoral induction was performed and mice were considered as no treated tumor survival group. In group 3 (DMH-PsAE), 8 weeks after tumor inductions started, by dilution of PsAE in the drinking water, animals were treated at the indicated dose. In group 4 (DMH-5Fu), 8 weeks after tumor inductions started, animals receive 5Fu as described before. In the current experiment, the human endpoints to decide the animals' euthanasia, were: anal bleeding, anal tumor protrusion, reduction of spontaneous activity, not eating/drinking, diarrhea, weight change more than 20 %, no micturition and dyspnea.

To study PsAE effects in allograft melanoma tumors, 3 groups of 10 C57BL6wt males, bred in our Institute, 6 weeks old, were used. In all groups, melanoma tumors were induced by subcutaneous inoculation of 1×10^5 B16-F0 (murine melanoma cancer cell line) in the right flank. Group 1, did not receive any treatment after tumor cells inoculation; groups 2 and 3, simultaneously with the tumor induction, animals received PsAE and 5Fu as was described previously. The animals were sacrificed at day 22 after cells inoculation. Then, developed tumors were dissected, measured, weighted, stored at -80 °C for immunobloting and fixed for histology.

All procedures were approved by the Institutional Animal Care and Use Committee of School of Medical Science, Universidad Nacional de Cuyo (Protocol approval N° 30/2014 and N° 103/2017, respectively). All animals in the protocols were cared in accordance with the Guiding Principles in the Care and Use of Animals of the US National Institute of Health.

4.4. Cell culture and in vitro treatments

Because, there is not available commercial mice colorectal cancer cell lines, the B16-F0 (ATCC, Virginia, EEUU) mice melanoma cell line was selected to perform the *in vitro* studies and to correlate with the *in vivo* findings. The cells were cultured as a monolayer in DMEM (Gibco, Grand Island, NY, USA), containing 10 % v/v fetal bovine serum (Hyclone, Canada), penicillin (100 IU/ml), streptomycin (100 μg/ml) and 3.7 mg/ml $NaHCO_3$. All cells were grown in a humidified atmosphere, containing 5% CO_2 at 37 °C. The treatments were dissolved in the culture media 24 h after cell plating. The chemotherapeutic agent 5Fu (Filaxis®, Argentina) was used as positive control at the indicated doses.

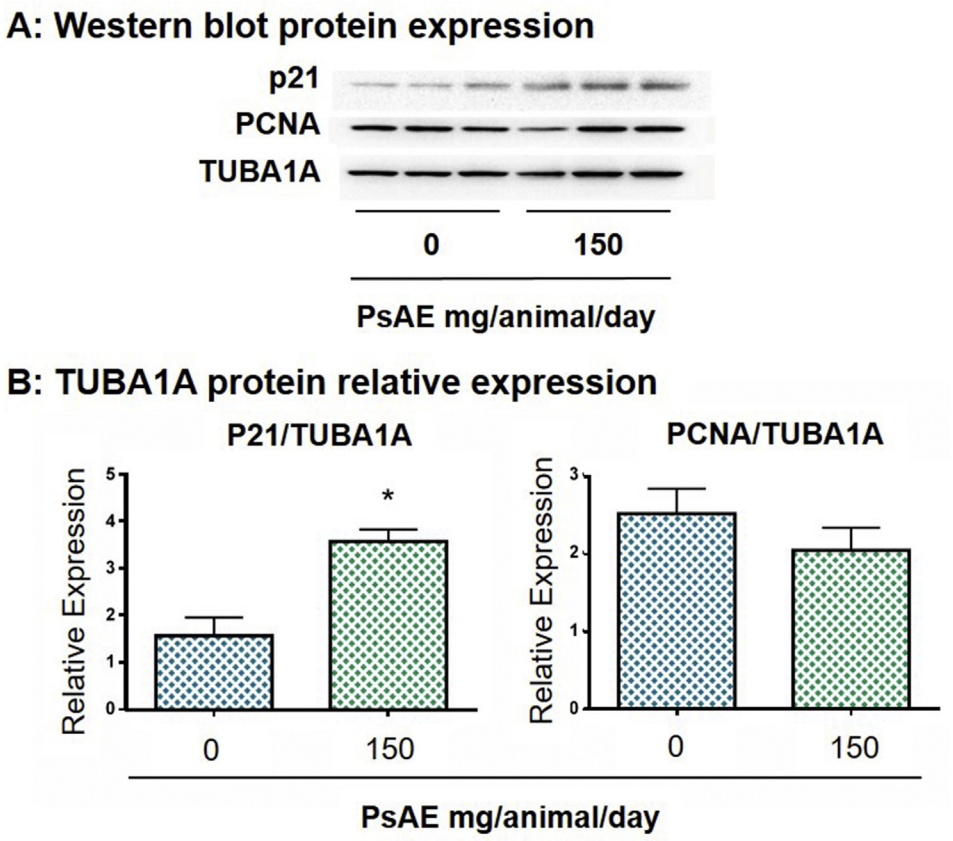

Figure 7. Western blot analysis of melanoma tumors. A. After 22 days of tumor induction, control and PsAE treated (150 mg/animal/day) groups are presented. B. Relative expression of p21 and PCNA over TUBA1A are expressed in terms of mean ± SEM. Results were compared by Student T test. *: indicates p = 0.0296. Full, non-adjusted images of p21 blot is provided in Supplementary Figure 5; TUBA1A (upper line) and PCNA (lower line) are provided in Supplementary Figure 6.

4.5. Dye exclusion assay

To quantify proliferation and viability, trypan blue exclusion assay was used in a dose-response experimental design. Briefly, 3×10^4 cells were seeded into 6-well plates. After 24 h, media was replaced with fresh culture media containing treatments at the indicated doses. After 48 h, total cells were collected by trypsinization, incubated with trypan blue and counted in a Neubauer haemocytometer chamber using a clear-field microscopy. To assess the IC_{50} (concentration of treatment that induces 50% of growth inhibition) and the LC_{50}, (concentration of treatment that induces 50% of lethality), the total cell number and death cells were used to statistically calculate the indexes (see below, point 2.11).

4.6. MTT cell proliferation assay

The MTT [(3-(4,5-dimethylthiazol-2-yl)-2,5-diphenyl tetrasodium bromide)] is a colorimetric assay for assessing cell metabolic activity. It is based on the cleavage of the yellow tetrazolium salt, MTT, to form a soluble blue formazan product by mitochondrial enzymes, and the amount of formazan produced is directly proportional to the number of viable cells present. In 96-well microplates, 7 10^3/100 μl B16-F0 cells were seeded; after 24 h, the medium was changed by fresh medium containing PsAE or 5Fu (Filaxis®, Argentina) at indicated doses. 48 h later, medium was replaced by MTT solution (0.5 mg/ml in DMEM, without phenol red nor FBS, 100 μl/well). Then, plates were incubated for an additional 4 h. After MTT solution was removed, 100 μl of DMSO were added to dissolve the formazan crystals and shaken for 10 min. To measure the optical density a Thermo Scientific Multiscan Elisa reader was used at 570 nm. The optical density obtained in untreated control cells (treatment concentration: 0 μg/ml) was considered as 100% viability; and the other values were calculated in accordance. The assay was performed three times in triplicate.

4.7. Proliferative responses by CFSE dilution

For examining cells proliferative activity, a cell tracking dye carboxyfluorescein diacetate succinimidyl ester (CFDASE) was used. In the labeled cells, the marker diffuses in the cytoplasm were present acetate groups are cleaved to a CFSE, a fluorescent derivative which remains into the cell. After mitosis, CFSE fluorescence intensity is divided in a half with each generation and the number of rounds of cell division can be visualized and quantified. Changes in CFSE fluorescence profile allows to determine changes in cell division induced by any substance. Decreased fluorescent intensity indicates higher proliferation rate; conversely, an increased in fluorescence intensity indicates lower/null proliferation. In the current assay, B16-F0 cells were stained with 5 μM of CFSE Cell Tracer Kit (Invitrogen) for 5 min at 37 °C. Then, labeled cells were washed, quantified and seeded at 5 10^4 well into a 6-well plates. Treatments at the indicated doses were performed for 48 h. Later, cells were scraped and acquired in a FACS Aria III flow cytometer (BD Biosciences, Mountain View, CA) and FlowJo.10 analysis software (Three star, US); Flow Jo proliferation tool was setting as follows: #peaks 4.00; Fixed ratio 0.66; fixed CV: 10.1; fixed backgd: 1087.0. All experiments were performed three times by triplicated.

4.8. Cell morphological analysis

Cells were seeded on cover-slides placed on the bottom of 6 well plates at a density of 3×10^4 cells/well and grown overnight. The next day, culture medium containing PsAE treatment was replaced at final concentrations of 0, 2.4 and 9 μg/ml; which represent control, IC_{50} and

$LC_{50,}$ respectively. After incubation for 48 h, the remaining cells were fixed with methanol and stained with crystal violet solution. Coverslides were then mounted, evaluated and photographed with a Nikon Eclipse 200 microscope.

4.9. Cell cycle assay

Into a 6 well/plate, 5×10^4 cells/well were seeded and grown overnight. Then, cells were treated with PsAE at 0 μg/ml, IC_{50} and LC_{50} concentrations, for 24 h. Later, cells were trypsinized, washed with PBS and fixed in 4% paraformaldehide overnight. Then, fixed cells were washed with PBS, incubated with 0.3 ml PBS containing 20 μg/ml RNase, 0.3 % IGEPAL, 1 mg/mL sodium citrate and 50 μg/ml of propidium iodide for 30 min at 37 °C. The population at each stage of the cell cycle was analyzed by flow cytometry, using a BD FACSaria III™ cytometer (BD Biosciences, Mountain View, CA) and FlowJo.10 analysis software (Three star, US).

4.10. Protein expression by western blot analyses

To determine protein expression, cultured B16-F0 cells were analyzed after 24 h of *in vitro* treatment. Melanomas generated *in vivo* by B16-F0 subcutaneous inoculation were also studied. Immunobloting was performed as described previously (Hapon et al., 2014). To quantify and statistically compares the protein expression, cultures were performed by triplicated and three melanomas group were studied. Primary antibodies used were: cyclin-dependent kinase inhibitor $p21^{cip1}$ (Termofisher AHZ0422), proliferating cell nuclear antigen (PCNA, Termofisher MA511358), caspase 3 (Casp3, Invitrogen, 74T2), cleaved poly (ADP-ribose) polymerase (cPARP, Termofisher 44698G), alpha tubulin (TUBA1A, Termofisher 322500). Peroxidase conjugate secondary antibodies used were: biotin conjugated antimouse and antirabbit (Jackson 115-035-003 and 711-065-152). Blots were developed using a ChemiDoc XRS + System (Bio-Rad, Laboratories) and band densitometric analysis was performed using Image Lab Software version 4.0 from Bio-Rad Laboratories.

4.11. Statistical analysis

All data are expressed as mean ± standard error (SEM) and analyzed using GraphPad Prism 6.0 software. The animal survival curves were performed by the Kaplan Meier analysis and compared using a Mantel Cox test. To assess IC_{50} and LC_{50}, was performed a sigmoidal dose-response analysis and, when the goodness of fit showed $R^2 \geq 0.90$, values were considered acceptable. When two groups were compared, the Student's T test was used; whereas, when more than two groups were compared, one-way ANOVA followed by Fisher LSD test was used. In all cases, statistical significance was considered when $p \leq 0.05$.

Declarations

Author contribution statement

Fabio Andrés Persia, Mariana Elizabeth Troncoso, Jorge Bórquez: Conceived and designed the experiments; Performed the experiments; Analyzed and interpreted the data.

Estefanía Rinaldini: Performed the experiments; Analyzed and interpreted the data.

Mario Simirgiotis, Alejandro Tapia, Juan Pablo Mackern-Oberti, María Belén Hapon, Carlos Gamarra-Luques: Conceived and designed the experiments; Performed the experiments; Analyzed and interpreted the data; Contributed reagents, materials, analysis tools or data; Wrote the paper.

Funding statement

This work was supported by 06/J473 and 06/M092 grants, from Secretaría de Ciencia, Técnica y Postgrado - Universidad Nacional of Cuyo – Argentina; PICT2014- 1877 grant, from Agencia Nacional de Promoción Científica y Tecnológica and Instituto Nacional del Cáncer grant, both from MINCyT - Argentina; and grant 11220150100579CO, from CONICET.

Competing interest statement

The authors declare no conflict of interest.

Additional information

Supplementary content related to this article has been published online at https://doi.org/10.1016/j.heliyon.2020.e03353.

Acknowledgements

We are indebted to María Emilia Gamarra-Hapon for the edition of the manuscript.

References

Asfour, M.H., Mohsen, A.M., 2017. Formulation and evaluation of pH-sensitive rutin nanospheres against colon carcinoma using HCT-116 cell line. J. Adv. Res. 9, 17–26.

Dolečková, I., Rárová, L., Grúz, J., Vondrusová, M., Strnad, M., Kryštof, V., 2012. Antiproliferative and antiangiogenic effects of flavone eupatorin, an active constituent of chloroform extract of *Orthosiphon stamineus* leaves. Fitoterapia 83, 1000–1007.

Dong, L., Xu, W.W., Li, H., Bi, K.H., 2018. *In vitro* and *in vivo* anticancer effects of marmesin in U937 human leukemia cells are mediated via mitochondrial-mediated apoptosis, cell cycle arrest, and inhibition of cancer cell migration. Oncol. Rep. 39, 597–602.

Gamarra-Luques, C.D., Goyeneche, A.A., Hapon, M.B., Telleria, C.M., 2012. Mifepristone prevents repopulation of ovarian cancer cells escaping cisplatin-paclitaxel therapy. BMC Canc. 12, 200.

Hapon, M.B., Hapon, M.V., Persia, F.A., Pochettino, A., Lucero, G.S., Gamarra-Luques, C., 2014. Aqueous extract of *Prosopis strombulifera* (Lam.) Benth. induces cytotoxic effects against tumor cell lines without systemic alterations in BALB/c mice. J. Clin. Toxicol. 4, 222.

Jiménez-González, A., Quispe, C., Bórquez, J., Sepúlveda, B., Riveros, F., Areche, C., Nagles, E., García-Beltrán, O., Simirgiotis, M.J., 2018. UHPLC-ESI-ORBITRAP-MS analysis of the native Mapuche medicinal plant "palo negro" (*Leptocarpha rivularis* DC. – Asteraceae) and evaluation of its antioxidant and cholinesterase inhibitory properties. J. Enzym. Inhib. Med. Chem. 33, 936–944.

Koyuncu, I., 2018. Evaluation of anticancer, antioxidant activity and phenolic compounds of *Artemisia absinthium* L. extract. Cell. Mol. Biol. (Noisy-le-grand) 64, 25–34.

Liu, W., Lu, Y., Chai, X., Liu, X., Zhu, T., Wu, X., Fang, Y., Liu, X., Zhang, X., 2016. Antitumor activity of TY-011 against gastric cancer by inhibiting Aurora A, Aurora B and VEGFR2 kinases. J. Exp. Clin. Canc. Res. 35, 183.

Malongane, F., McGaw, L.J., Mudau, F.N., 2017. The synergistic potential of various teas, herbs and therapeutic drugs in health improvement: a review. J. Sci. Food Agric. 97, 4679–4689.

Mamone, L., Di Venosa, G., Valla, J.J., Rodriguez, L., Gándara, L., Batlle, A., Heinrich, M., Juarranz, A., Sanz-Rodriguez, F., Casas, A., 2011. Cytotoxic effects of Argentinean plant extracts on tumour and normal cell lines. Cell. Mol. Biol. (Noisy-le-grand) 57 (Suppl), OL1487–1499.

Moreno-Sánchez, R., Marín-Hernández, A., Saavedra, E., Pardo, J.P., Ralph, S.J., Rodríguez-Enríquez, S., 2014. Who controls the ATP supply in cancer cells? Biochemistry lessons to understand cancer energy metabolism. Int. J. Biochem. Cell Biol. 50, 10–23.

Navarro, M., Moreira, I., Arnaez, E., Quesada, S., Azofeifa, G., Vargas, F., Alvarado, D., Chen, P., 2017. Flavonoids and ellagitannins characterization, antioxidant and cytotoxic activities of *Phyllanthus acuminatus* Vahl. Plants 6 pii E62.

Persia, F.A., Rinaldini, E., Carrión, A., Hapon, M.B., Gamarra-Luques, C., 2017. Evaluation of cytotoxic and antitumoral properties of *Tessaria absinthioides* (Hook & Arn) DC, "pájaro bobo", aqueous extract. Medicina 77, 283–290.

Persia, F.A., Rinaldini, E., Hapon, M.B., Gamarra-Luques, C., 2016. Overview of genus *Prosopis* toxicity reports and its beneficial biomedical properties. J. Clin. Toxicol. 6, 326.

Radan, M., Carev, I., Tešević, V., Politeo, O., Čulić, V.Č., 2017. Qualitative HPLC-DAD/ESI-TOF-MS analysis, cytotoxic, and apoptotic effects of Croatian endemic *Centaurea ragusina* L. aqueous extracts. Chem. Biodivers. 14.

Rashid, H., Gafur, M.A., Sadik, G., Rahman, A.A., 2002. Biological activities of a new derivative from *Ipomoea turpithum*. Pakistan J. Biol. Sci. 5, 968–969.

Ravindranath, M.H., Muthugounder, S., Presser, N., Viswanathan, S., 2004. Anticancer therapeutic potential of soy isoflavone, genistein. Adv. Exp. Med. Biol. 546, 121–165.
Simirgiotis, M.J., Quispe, C., Areche, C., Sepúlveda, B., 2016. Phenolic compounds in Chilean mistletoe (Quintral, *Tristerix tetrandus*) analyzed by UHPLC-Q/Orbitrap/MS/MS and its antioxidant properties. Molecules 21, 245.
Singh, S., 2007. From exotic spice to modern drug? Cell 130, 765–768.
Sultana, S., Asif, H.M., Nazar, H.M., Akhtar, N., Rehman, J.U., Rehman, R.U., 2014. Medicinal plants combating against cancer: a green anticancer approach. Asian Pac. J. Cancer Prev. APJCP 15, 4385–4394.
Tremocoldi, M.A., Rosalen, P.L., Franchin, M., Massarioli, A.P., Denny, C., Daiuto, É.R., Paschoal, J.A.R., Melo, P.S., Alencar, S.M., 2018. Exploration of avocado by-products as natural sources of bioactive compounds. PloS One 13, e0192577.
Tsao, S.M., Hsia, T.C., Yin, M.C., 2014. Protocatechuic acid inhibits lung cancer cells by modulating FAK, MAPK, and NF-κB pathways. Nutr. Canc. 66, 1331–1341.
Wang, J., Fang, X., Ge, L., Cao, F., Zhao, L., Wang, Z., Xiao, W., 2018. Antitumor, antioxidant and anti-inflammatory activities of kaempferol and its corresponding glycosides and the enzymatic preparation of kaempferol. PloS One 13, e0197563.
Wang, H.C., Pao, J., Lin, S.Y., Sheen, L.Y., 2012. Molecular mechanisms of garlic-derived allyl sulfides in the inhibition of skin cancer progression. Ann. N. Y. Acad. Sci. 1271, 44–52.
Yu, X., Liang, Q., Liu, W., Zhou, L., Li, W., Liu, H., 2017. Deguelin, an Aurora B kinase inhibitor, exhibits potent anti-tumor effect in human esophageal squamous cell carcinoma. EBioMedicine 26, 100–111.
Zhang, X., Dwivedi, C., 2011. Skin cancer chemoprevention by α-santalol. Front. Biosci. (Scholar Ed.). 3, 777–787.
Zhao, Z., Jin, G., Yao, K., Liu, K., Liu, F., Chen, H., Wang, K., Gorja, D.R., Reddy, K., Bode, A.M., Guo, Z., Dong, Z., 2019. Aurora B kinase as a novel molecular target for inhibition the growth of osteosarcoma. Mol. Carcinog. 58, 1056–1067.